FRICTION MODELLING OF A LINEAR HIGH-PRECISION ACTUATOR

J. Zimmermann[1], O. Sawodny[1], T. Hausotte[2], G. Jäger[2]

[1]*Technische Universität Ilmenau, Institute for Automation and Systems Engineering, P.O. Box 100 565, D-98684 Ilmenau, Germany*
[2] *Technische Universität Ilmenau, Institute of Process Measurement and Sensor Technology, P.O. Box 100 565, D-98684 Ilmenau, Germany*

Abstract – For control applications aiming accurate positioning and path tracking friction modelling and compensation can be very important, especially when working with small displacements as usual in nano technologies. The paper at hand describes friction identification and friction model application for a linear high-precision ball bearing guide driven by a voice coil actuator and using high-resolution position measurement equipment. After noting some friction models the characteristics of friction on nanometer scale are investigated with several experiments. At last some remarks on control design are given.

Keywords: friction models, friction identification, high resolution measuring

1. INTRODUCTION

Miniaturisation in advanced technologies demands for high-precision measuring and positioning concepts and machines. The high resolution does not exclude but complicates a large operating range. This paper is about friction modelling on the nanometer scale and summarises results from a research work supported by the Department of Control Engineering and the collaborative research centre SFB 622 'Nanopositionier- und Nanomessmaschinen' of the Technische Universität Ilmenau. The currently developed Nano Measuring and Positioning Machine has an operating range of 25mm x 25mm x 5mm. It is capable of 0.1nm resolution for measurements and allows positioning steps below 1nm (Hausotte 2002; Hausotte, *et al.* 2004). This extraordinary accuracy is reached by an Abbe offset-free design in conjunction with a corner mirror serving as reference coordinate system. Depending on the application high precision positioning and/or exact path-tracking is required. Therefore the nonlinear behaviour of friction is one important aspect to understand for control design. After discussing some friction models and visualising the test bed, some investigations and experiments related to friction modelling of a linear roller bearing guide are presented. Before taking conclusions a short look on control aspects and simulation of friction models is given.

2. FRICTION MODELS

There is a wide range of literature dealing with frictional phenomena from different considerations and for various applications. This study is designed for systems engineering and does not deal with physical background of the dynamic behaviour, but uses the idea of models.

2.1 Static Models

The simplest way of friction modelling is the 'Coulomb model' using equation 1. The friction force depends on surface conditions represented by μ and the normal force between the two involved surfaces. When applying an external force smaller than the Coulomb force, then there is no movement and the friction force is equal to the affecting one.

$$F_f = \operatorname{sgn}(\dot{x}) \cdot F_C = \operatorname{sgn}(\dot{x}) \cdot \mu \cdot F_N \qquad \dot{x} \neq 0 \qquad (1)$$

This model is rather simple and the signum function may lead into numerical problems when simulating.

An extension to this model is a velocity dependent part of friction, which can be explained by a viscosity of the lubricating film between the two surfaces.

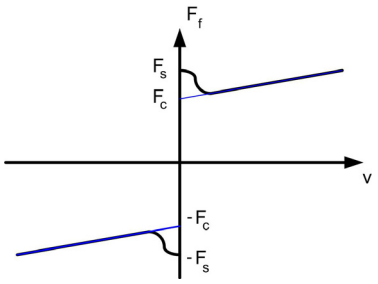

Fig. 1. Stribeck curve

Since the thickness of the lubricant film decreases during standstill periods, the force required for breakaway may be larger than the one for moving slowly having a small film. The influence of viscosity under higher velocities depends on the material combination including lubricant and is reflected by the macro-viscose damping factor σ_2. The evolving Stribeck curve is shown exemplary in figure 1. The Stribeck force is present for breakaway and can be found near zero velocity. The Stribeck velocity v_S can be found around the minimum of the friction force, Canudas de Wit (1995) used a normal probability curve to model the Stribeck curve and therefore assumed that the friction force at Stribeck velocity is decreased to around 37% of the Stribeck overshot $F_S - F_C$.

2.2 *Dynamic Models*

All of these static models are able to roughly reflect the real dynamic behaviour, but modelling on nanometer scale demands for a more precise description. There are some extensions like dynamic models from Dahl (Dahl 1968) and Bliman-Sorine. These are able to reflect some pre-sliding and hysteresis related phenomena. An extensive discussion of these models including their properties and implementation is given for instance by Guran, *et al.* (1996), and Åström, *et al.* (1998).

Bristle Models. Another class of dynamic models are the single state bristle friction models. They are based on the idea that the surface of all objects is rough and the small elevations of the loaded contact are acting like elastic bristles (Haessig and Friedland 1990). The visualisation of bristle properties is shown in figure 2. When moving the two interacting surfaces relatively to each other, then the bristles are deflecting and may also slide through. As a result the state of the model is the variable z which can be interpreted as the average bristle deflection. In order to limit the number of states, the bristles of one side are thought to be stiff. The flexible bristles of the model are mapped with spring and damper in parallel, and their maximum deflection is limited.

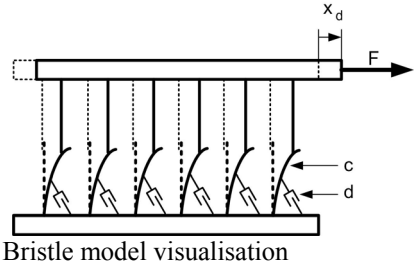

Fig. 2. Bristle model visualisation

Beginning in initial position both pairs of bristles are standing straight. When applying a small force in parallel to the contact then there is a small displacement. As a result the bristles of one side are deflecting and thereby energy is stored within the spring and transformed within the damper. After the maximum bristle deflection is reached and the force is still increasing both pairs of bristles are slipping over, but the bristle deflection is held while the force is applied. Parameters of the abstract bristles are the micro elastic stiffness σ_0, the micro plastic damping σ_1 and the maximum bristle deflection z_{ss}.

2.3 *LuGre Model*

The LuGre model was introduced by Canudas de Wit, *et al.* (1995), using equations (2) to (4). The friction force is assembled of a spring and a damper force caused by the bristle deflection and a micro viscose velocity dependent damping. The function $g(\dot{x})$ represents the Stribeck curve using an e-function. In addition the dynamic behaviour in form of the slipping bristles is introduced by the state variable z. Small forces below Coulomb force cause mainly elastic and less plastic displacement leading into small permanent displacements, but elastic and plastic attributes are always combined. When applying a periodical unidirectional force with amplitude below Stribeck force, then the model predicts non-physical absolute displacement. A force with an amplitude above the Stribeck force causes an absolute movement with increasing or decreasing friction, defined by the used lubricant and represented by the parameter σ_2.

$$F_f = \sigma_0 \cdot z + \sigma_1 \cdot \dot{z} + \sigma_2 \cdot \dot{x} \tag{2}$$

$$\dot{z} = \dot{x} - \frac{|\dot{x}|}{g(\dot{x})} \cdot z \tag{3}$$

$$g(\dot{x}) = \frac{1}{\sigma_0}\left[F_C + (F_S - F_C) e^{-\left(\frac{\dot{x}}{v_S}\right)^2} \right] \tag{4}$$

The LuGre model captures many aspects of friction, but allows no further modelling of the pre-sliding domain. In addition the model can become unstable or violate passivity, which can be handled by choosing suitable parameters, see Canudas de Wit (1998) and Barabanov and Ortega (2000). An extensive discussion of the LuGre model in comparison to classical models can be found in Åström, *et al.* (1998).

2.4 *Elasto-plastic Model*

While the LuGre model assumes that plastic and elastic displacements are always combined, the elasto-plastic model enables precise modelling of the pre-sliding domain and the dynamic transition to sliding domain. The model was introduced by Dupont, *et al.* (2002) and is described by equations

(5) to (8) and (9). On a displacement below the breakaway distance z_{ba} of the bristles only elastic displacement occurs. Further deflection causes a varying mix of elastic and plastic displacement until the maximum deflection z_{ss} is reached. Further increase of the applied force into the same direction causes plastic sliding connected with the elastic deflection held while the force is applied.

$$F_f = \sigma_0 \cdot z + \sigma_1 \cdot \dot{z} + \sigma_2 \cdot \dot{x} \tag{5}$$

$$\dot{z} = \dot{x} \cdot \left(1 - \alpha(z,\dot{x}) \frac{z}{z_{ss}(\dot{x})} \right) \tag{6}$$

$$\alpha(z,\dot{x}) = \begin{cases} 0 & |z| \le z_{ba} \\ 0 < \alpha_m < 1 & z_{ba} < |z| < z_{ss}(\dot{x}), \operatorname{sgn}(\dot{x}) = \operatorname{sgn}(z) \\ 1 & |z| \ge z_{ss}(\dot{x}), \operatorname{sgn}(\dot{x}) = \operatorname{sgn}(z) \\ 0 & \operatorname{sgn}(\dot{x}) \ne \operatorname{sgn}(z) \end{cases} \tag{7}$$
$$0 < z_{ba} < z_{ss}(\dot{x})$$

$$\alpha_m(z) = \tfrac{1}{2} \sin\left(\pi \frac{z - \frac{z_{ss}+z_{ba}}{2}}{z_{ss} - z_{ba}} \right) + \tfrac{1}{2} \quad \text{with} \quad z_{ba} \le |z| < z_{ss} \tag{8}$$

$$z_{ss}(\dot{x}) = \frac{\operatorname{sgn}(\dot{x})}{\sigma_0} \left[F_C + (F_S - F_C) e^{-\left(\frac{\dot{x}}{v_S}\right)^2} \right] \tag{9}$$

The function $\alpha(z,\dot{x})$ defines the transition from plastic into the elasto-plastic domain of the model and reflects the bristle model properties. This includes pre-sliding displacement and the Stribeck effect. As a result the maximum bristle deflection $z_{ss}(\dot{x})$ depends on velocity in order to reflect the Stribeck curve, for example equation (9) from Canudas de Wit, *et al.* (1995), can be utilized. The function $\alpha_m(z)$ describes the allocation of the elastic and elasto-plastic domain, when the direction of bristle deflection is equal to the overall test bed moving direction. If $\alpha = 0$ then there is only elastic displacement causing the object to come back to the initial point when throttling the applied force to zero. For $\alpha = 1$ the bristles are deflected to their maximum and there is large absolute movement leading into a permanent displacement. All intermediate values are describing the transition from elastic into elasto-plastic movement.

3. EXPERIMENTAL SETUP

For experiments with the system one axis composed of a linear voice coil actuator from BEI-KIMCO and a ball bearing guide with an operating range of 25mm was utilized. The test bed was build up with parts from a Nano Measuring and Positioning Machine (Hausotte 2002). The experiment board is a heavy weight metal slab located on a damping table, shown in figure 3. The actuator is driven using an amplifier controlled by a DSPACE PowerPC or an Innovative Integrations M44 microcontroller.

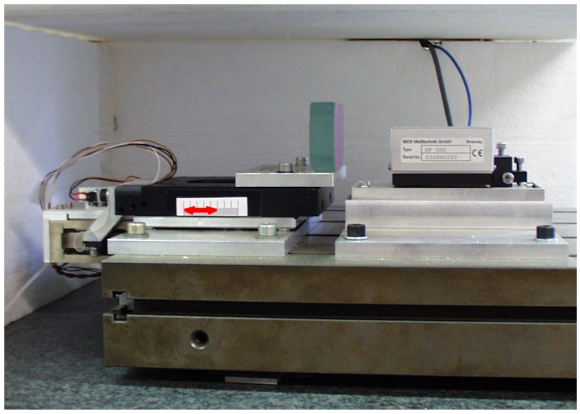

Fig. 3. Experimental setup

Since the actuator introduces no friction the investigated effects are introduced by the mechanical guide. For system control, data acquisition and processing a dSPACE system using MATLAB/Simulink was deployed. The measurement and control systems are working synchronized with a sampling rate of 6.25 kHz.

Position Measurements. High resolution position measurement is obtained by using a laser interferometer including suitable data correction and pre-processing methods implemented on a micro controller, described in detail by Hausotte (2002). The interferometer is a modified SP-500 of SIOS (SIOS 2004) which has a resolution of below 0.1nm. Finally the calculated position is transferred into the DSPACE system, where velocity and acceleration are calculated after the measurement was filtered.

Friction Force Calculation. Since the actuator parameters are known, the force resulting from an applied current can be calculated. Therefore the actuator current is measured with the DSPACE system using a sensor resistor connected with a measuring amplifier. The filtered measurements are corrected using the overall characteristics of the measuring section and the actuator. The acceleration force can be defined based on calculated acceleration values. Finally, the balance of forces was used to define the disturbed values of the friction force.

3.1 System Identification

System identification starts with parameters of the mechatronic system as the mass of the moveable parts of the roller bearing guides and general actuator parameters. The specified parameters are utilized for another series of measurements. Following experiments are related to friction phenomena and carried out with the open loop system using test functions. Referring to the elasto-plastic model the three domains of friction are investigated.

Elastic Domain. The elastic domain is present for small amplitudes of applied force and small displacements. In order to examine this behaviour test functions with small amplitude are utilized. A ramp like function deflects towards one direction before throttling the force to zero and deflecting towards the opposite direction.

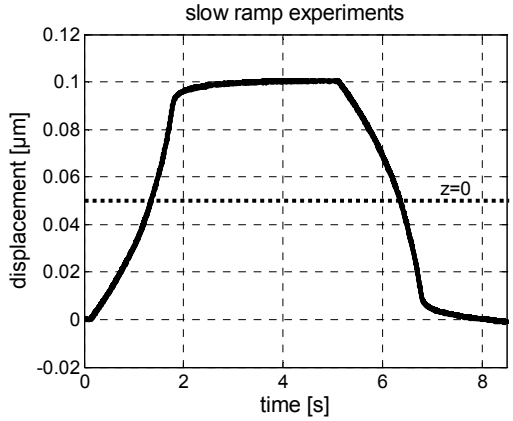

Fig. 4. Elastic displacement – ramp function

The maximum friction force is around half of the Coulomb force of approximately 400mN. Figure 4 shows that there is only a small additional displacement after the maximum force was reached, which illustrates the mostly elastic behaviour. Next experiments are using a periodic actuator force in order to compare the reaction on different frequencies. Figure 5 shows friction force as a function of displacement when working with an actuator force of 250mN and a frequency of 1Hz or 10Hz applied to the system. While the first frequency causes a displacement with maximal amplitude of approximately 50nm, the second one only reaches a value of approximately 40nm. This behaviour is characterised by the bristle spring and damper system of the model causing a higher damper force when working with larger velocities. This points out that the stiffness of the elastic domain should be investigated with small amplitudes and frequencies. The influence of the damping is already noticeable when working with small displacements. In addition figure 6 shows normalised friction force and normalised velocity as a function of time when working with a frequency of 1Hz. The maximum velocity is around 0.6µm per second. For comparison figure 7 shows the same details when applying an external force with a frequency of 10Hz causing a maximum velocity of 3µm per second. In both cases the friction force is around its maximum near zero velocity, but the force at maximum velocity depends on the frequency of the applied force. The shown velocity curve is not symmetric to its maximum but releases faster than it rises.

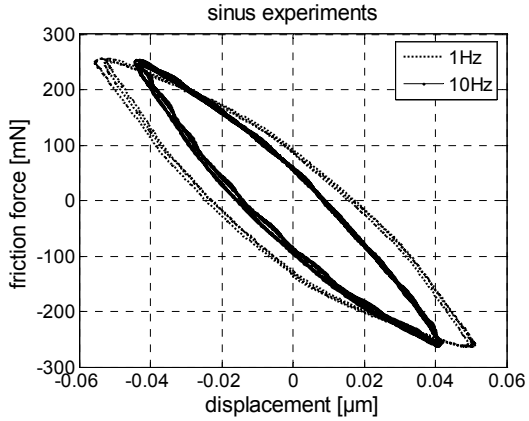

Fig. 5. Periodic force 1Hz/10Hz 250mN

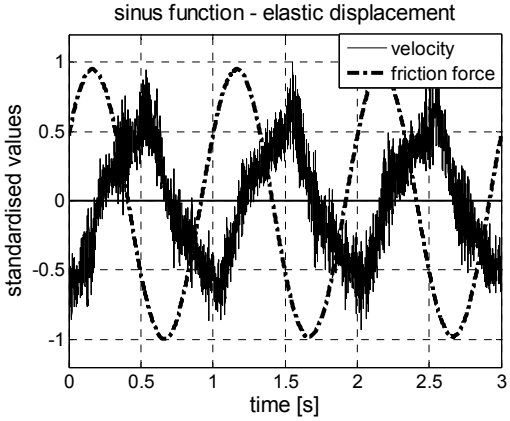

Fig. 6. Sinus 1Hz friction force and velocity

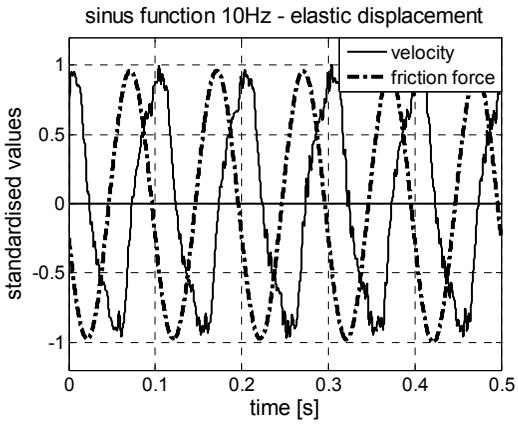

Fig. 7. Sinus 10Hz friction force and velocity

This behaviour can partly be explained with the micro plastic damping, but also effects like the frictional lag including the influence of the force build-up time (Åström, *et al.* 1998) are present. The LuGre model partly reflects this behaviour better than the elasto-plastic model, which leads to the assumption that the mixture of elastic and plastic displacement may also depend on the rate of the applied force.

Elasto- Plastic Domain. In order to find out more about the transition from elastic to plastic domain larger amplitudes of force are applied to the system. A function with dwell times among ramps of maximal amplitude around Coulomb friction is utilized. Figure 8 shows the resulting friction force as a function of displacement.

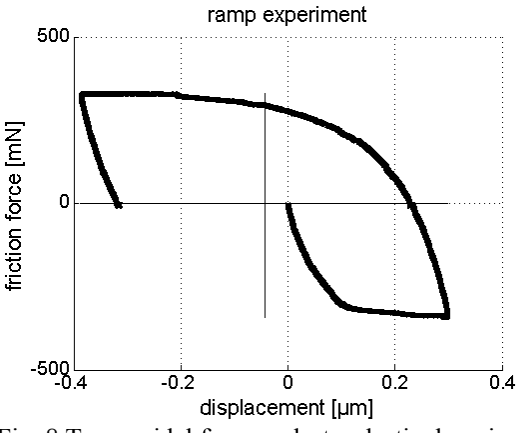

Fig. 8 Trapezoidal force – elasto-plastic domain

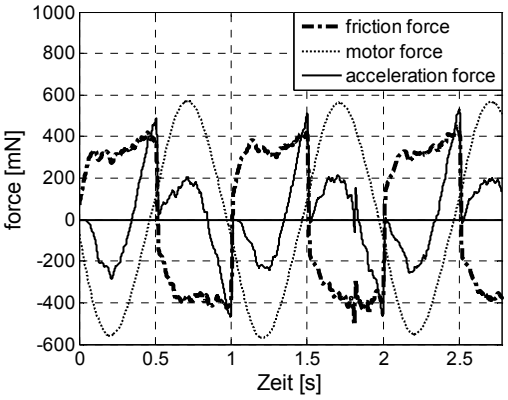

Fig. 9. Large displacement – forces

The displacement is increasing with the applied force, but within the first domain below 100nm less fast than above this limit. There is only small additional displacement before the force starts throttling. When decreasing the force to zero also the displacement decreases by 100nm in total. The ramp into the opposite direction shows similar behaviour, but the absolute displacement is much bigger. This is caused by direction dependent friction parameters and maybe also by the lubricating film that was built up during movement after the experiment started in hold-up state.

(Mostly) Plastic Domain. In addition experiments with higher forces and velocities are conducted. As mentioned before the elastic properties still remain during large plastic movements.
The test bed provides only a small operating range which complicates conducting exact experiments over the whole range, since there must be enough room for acceleration and deceleration phases. This restriction does not affect the results for this application, because normally only small velocities appear. Anyway this limits the possibility to investigate the velocity dependent part of friction, which can be seen well with large linear or circular setups.
Figures 9 to 10 show results of an experiment using a periodic actuator force with amplitude above Coulomb friction. As a result there is a large displacement and a maximum velocity of 4 cm per second is reached. For identification of the Stribeck curve Åström, *et al.* (1998), arranged several experiments using different but steady velocities.

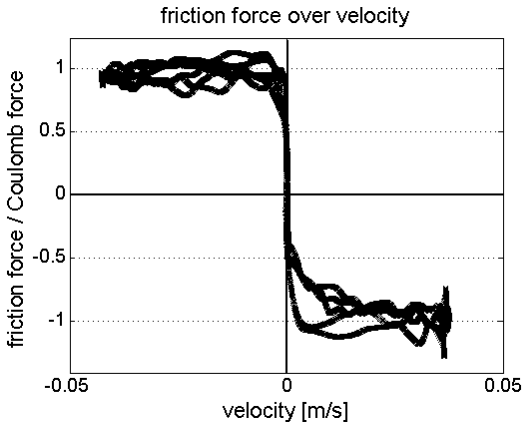

Fig. 10. Large periodical displacement – friction force as a function of velocity

Since the operating range complicates these experiments much and the application does not require the model to capture this area of operations, the curve resulting from one experiment is shown in figure 11. The friction force is shown as value relative to the Coulomb force because it depends on position and moving direction. The curve exhibits that the force for acceleration is smaller than the one for deceleration. In addition there is nearly no macro viscose damping, resulting in $\sigma_2 \approx 0$.

Dynamic Parameters. Additional complexity is introduced since friction parameters are depending on position and moving direction. In order to take this behaviour into account lookup tables can be used. A position dependent Coulomb force can be incorporated into the model by modifying the maximum bristle deflection, which causes deviant behaviour for small displacements between large movements. Another method may modify σ_0 depending on position and moving direction, but this involves also the adaptation of σ_1 in order to keep the spring damper ratio. The reflection of dwell time dependent friction force may be hard, because it is position and course dependent. Furthermore, other disturbances from outside or inner stress are affecting the overall positioning much more. In addition to the influence of temperature and humidity also impact sound and airborne sound are influencing the overall operation of the test bed. Anyway an implementation would support model based investigation of effects.

Aspects for Control Design. Since the application of nano positioning uses mostly small displacements and velocities, reflection of the elasto-plastic domain is fundamental. In Dupont, *et al.* (2002b), a discrete, time free friction force calculator for the elasto-plastic model is introduced. In comparison to the LuGre observer (Canudas de Wit, *et al.* 1995) this one offers a more precise emulation of small movements and simply provides numerical stability. This type of observer without feedback uses only the position and velocity values to estimate the actual friction force, which requires suitable position measurement frequency and resolution. As a result it is stable and does not exhibit non-physical drift like the LuGre model may do when applying small unidirectional periodical forces. In some cases complex actions may also lead into friction force errors caused by a bristle deflection divergence. In addition to resetting the bristle reflection under special conditions, also an extra observer can be utilized for force adaptation. The simplest way of implementation is a closed loop Coulomb force observer that adapts the elasto-plastic observer. The currently implemented control system of the Nano Measuring and Positioning Machine is characterised in Hausotte, *et al.* (2004). For fine positioning a PID controller with some modifications and adapted characteristics is implemented. Since the application of three dimensional positioning requires a configuration of three axes, dynamic coupling effects must be considered (Tien, *et al.* 2004; Hausotte 2002).

4. SIMULATION

The parameters of the friction models are identified using several experiments like shown above. Since some parameters depend on position as well as on moving direction, the given values are based on scripts aimed at an automatic examination of performed experiments. In addition optimisation techniques are applied to adapt the model parameters. Based on the conducted experiments several simulation runs using the LuGre and the elasto-plastic model are applied to a model of the system in order to find a reasonable choice for further experiments and research. Figure 11 compares a measurement with simulation runs for applying the measured actuator force including noise.

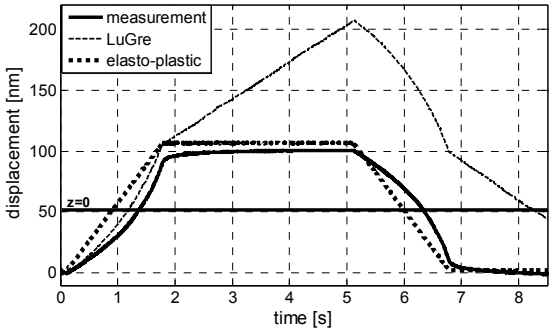

Fig. 11. Friction models – elastic domain (cp. Fig. 4)

Table 1: Friction model parameters

	elasto-plastic	LuGre
F_c [mN]	400	400
σ_0 [N/m]	4000000	4270000
σ_1 [N s/m]	4170	4730
σ_2 [N s/m]	0	0
z_{ss} [nm]	100	100
z_{ba} [nm]	50	--
F_s [mN]	400	400
v_s [m/s]	0,0007	0,0007

The parameters of the friction models used for simulations are shown in Table 1. The elasto-plastic model reflects the pre-sliding domain more accurate than the LuGre model, because the transition from elastic into the elasto-plastic domain can be modelled in detail. Furthermore, the model reacts less sensible to the effect of noise (Fig. 11). Large movements are realistically reflected by both models.

5. CONCLUSIONS

The LuGre model and the elasto-plastic model are applied to a linear high-precision ball bearing guide. Both models capture the main aspects of friction, but the elasto-plastic model describes pre-sliding movements more accurate than the LuGre model, which is important on nanometer scale. Both friction models enable further computer based analysis and model based optimisation in order to polish positioning and tracking characteristics of the control system. In any case the control system must be able to react on disturbances since the exact developing of friction values may vary. Further adaptation of the elastic properties and the transition from elastic into the elasto-plastic domain are extensions of this work.

Acknowledgements

The collaborative research centre SFB 622 'Nanopositionier- und Nanomessmaschinen' is supported by the German Research Foundation (DFG) and the Thuringian Ministry of Science, Research and Arts. The authors would like to thank all those colleagues who have contributed to the developments described.

References

Åström, K. J.; Canudas de Wit, C.; Olsson, H.; Gäfvert, M.; Lischinsky, P. (1998). Friction Models and Friction Compensation. *European Journal of Control*, **Vol. 29(4)**, pp. 176- 195

Canudas de Wit, C.; Olsson, H.; Åström, K. J.; Lischinsky, P. (1995). A new Model for Control of Systems with Friction. *IEEE Transactions on Automatic Control*, **Vol. 40(3)**, pp. 419-425

Canudas de Wit, C. (1998). Comments on "A new Model for Control of Systems with Friction". *IEEE Transactions on Automatic Control*, **Vol. 43(8)**, pp. 1189-1190

Barabanov, N.; Ortega, R. (2000). Necessary and Sufficient Conditions for Passivity of the LuGre Friction Model. *IEEE Transactions on Automatic Control*, **Vol. 45(4)**, pp.830-832

Dahl, P. (1968). A solid friction model. , *Tech. Report TOR-0158(3107-18)-1*, Aerospace Corp., El Segundo, Ca.

Dupont, P.; Armstrong, B.; Hayward, V.; Altpeter, F. (2002a). Single State Elastoplastic Friction Models. *IEEE Transactions on Automatic Control*, **Vol. 47(5)**, pp.787-792

Dupont, P.; Armstrong, B.; Hayward, V. (2002b). Single State Elastoplastic Friction Models for Friction Compensation. *IEEE Transactions on Automatic Control 2001,* Article TP99-255 Revision 2002

Guran, A.; Pfeiffer, F.; Popp, K. (1996). Dynamics with Friction: Modeling, Analysis and Experiment. *Part I & II; Stability, Vibration and Control of Systems*, **Series B Volume 7**, World Scientific Publishing Singapore

Haessig, D.; Friedland, B. (1990). On the modelling and simulation of friction. *Proceedings of the ACC San Diego 1990,* pp. 1256-1261

Hausotte, T. (2002). *Nanopositionier- und Nanomessmaschine*. Dissertation, Technische Universität Ilmenau

Hausotte, T.; Jäger, G.; Manske, E.; Sawodny, O. (2004). *Control System of a nanopositioning and nanomeasuring machine*. Proceedings Actuator 2004 pp. 123-126

SIOS Meßtechnik GmbH (2004). *www.SIOS.de*, Ilmenau/ Germany

Tien, Szuchi; Zou, Quingze; Devasia, S. (2004). *Iterative Control of Dynamics-Coupling Effects in Piezo-based Nano-Positioners for High-Speed AFM*, Proceedings IEEE 2004, pp. 711-717